Quantum cluster approach to the topological invariants in correlated Chern insulators

Zhao-Long Gu [1], Kai Li[1], and Jian-Xin Li[1,2]

[1] National Laboratory of Solid State Microstructures and Department of Physics, Nanjing University, Nanjing 210093, China
[2] Collaborative Innovation Center of Advanced Microstructures, Nanjing University, Nanjing 210093, China

E-mail: `jxli@nju.edu.cn`

Abstract.
    We detect the topological properties of correlated Chern insulators with strong Coulomb interactions by use of cluster perturbation theory and variational cluster approach. The common scheme in previous studies only involves the computation of the interacting bulk Chern number by means of the so-called topological Hamiltonian. With close investigations on a prototype model, the half-filled Haldane Hubbard model, which is subject to both periodic and open boundary conditions, we uncover the unexpected failure of this scheme due to the explicit breaking of the translation symmetry that is universal in most quantum cluster methods. We assert that a faithful verification of a nontrivial topological phase in correlated Chern insulators by quantum cluster approaches must combine a nonzero interacting bulk topological invariant and the existence of gapless states or zero-energy zeros of the single particle Green's function on edges.

1. Introduction

Band insulators with nontrivial topology have become one of the central interests in condensed matter physics since the discovery of topological insulators [1, 2]. Beyond the traditional Landau paradigm, topological insulators cannot be distinguished from ordinary ones by local order parameters, but are featured by gapless edges states on open boundaries [3, 4, 5, 6, 7, 8]. The existence of such edge modes is linked to the emergence of nonzero topological invariants of the bulk energy bands via the bulk-edge correspondence [9]. Thus the identification of a topological invariant is of particular importance to characterize different phases of band insulators. Indeed, in terms of such topological invariants constructed from the free Hamiltonians, a complete classification has been developed for non-interacting systems in different symmetry classes [10].

The presence of strong interactions between electrons enriches the physics of topological bands, and brings many challenges to this area at the same time. One of such demanding questions is how one can compute the topological invariant in a interacting system. A pioneering work by Volovik [11] expresses the Chern number [12] of a two dimensional Chern insulator in terms of the single particle Green's functions. This formula is ready to be generalized to deal with correlated Chern insulators by a simple substitution of the free propagator with the interacting one. A great simplification of this formula was proposed in Ref. [13] that the zero-energy single particle Green's function alone is sufficient to calculate the interacting Chern number via the Kubo formula. Later, the concept of the so-called topological Hamiltonian [14], i.e. the minus inverse of the dressed single particle Green's function, was shown to apply equally in other systems with diverse topological classifications [15, 16, 17, 18, 19], such as the quantum spin Hall insulators [16, 17], topological superconductors [18], interacting Su-Schrieffer-Heeger chains [19], etc.

The success of the topological Hamiltonian relies on a credible computation of the interacting single particle Green's functions. In recent years a variety of quantum many-body algorithms gathering under the name of quantum cluster approaches [20, 21] have been developed to calculate such single particle Green's functions of a broad range of strongly correlated fermionic systems [22, 23, 24, 25, 26, 27, 28, 29, 30] and bosonic systems [31, 32, 33]. They share the basic idea of solving a reference system composed of isolated finite-sized clusters that are sometimes embedded in a uncorrelated bath media. They give access to nontrivial many body effects and can be unified within the variational principle based on the self energy functional approach [34]. These methods include cluster perturbation theory (CPT) [22], dynamical cluster approach (DCA) [23], cellular dynamical mean field theory (CDMFT) [24], variational cluster approach (VCA) [25], cluster dynamical impurity approximation (CDIA) [26], etc, and have been widely applied to detect the topological properties of interacting topological band insulators [28, 17, 35, 18].

In this article we focus on the scheme of applying quantum cluster approaches to the determination of topological invariants in correlated Chern insulators. The prototype

is the half-filled Haldane Hubbard model [36, 37, 38, 39, 40, 41, 42, 43, 44, 45, 46, 47], which exhibits quantum anomalous Hall effect with weak Coulomb interactions and is antiferromagnetically ordered in the strong coupling limit. Previous quantum cluster methods [35] predicted a topological Neel antiferromagnet and/or a topological nonmagnetic Mott insulator in the moderate interacting regime. These intermediate phases were claimed to be topological because their interacting bulk Chern numbers constructed from the topological Hamiltonians were shown to be nonzero. According to the generalized bulk-edge correspondence appropriate to correlated topological insulators [48, 49], there should exist gapless states or zero-energy zeros of the single particle Green's functions on open boundaries for these predicted phases. However, this self-consistency is seldom verified with an actual check in the common scheme of the quantum cluster approach community but is always argued to hold [35]. Unexpectedly, with close investigations on this model subject to both periodic and open boundary conditions, we find no such gapless modes or zero-energy zeros on the edges of these intermediate phases although the bulk interacting Chern number is confirmed to be nonzero in our CPT and VCA results. We attribute this paradox to the falsity of the bulk interacting Chern number and elaborate that this artifact arises from the explicit breaking of the translation symmetry that is universal in most quantum cluster approaches. Therefore, we assert that a faithful verification of the nontrivial topological property of correlated electron systems by quantum cluster approaches must combine a nonzero interacting bulk topological invariant and the existence of gapless states or zero-energy zeros of the single particle Green's function on edges.

The rest of the paper is organized as follows. In Sec. 2, we give a brief review on the Haldane Hubbard model and the CPT/VCA methods. In Sec. 3, we present the numerical results and elaborate the falsity of the calculated interacting bulk Chern number. Section 4 provides a summary and discussion.

2. Model and method

The Haldane Hubbard model is written as $H = H_0 + H_U$ as shown in Fig. 1(a), where H_0 is the spinful version of the Haldane model on the honeycomb lattice with the next-nearest-neighbor (NNN) hopping phase $\phi = \pi/2$[3],

$$H_0 = -t \sum_{\langle ij \rangle \sigma} c_{i\sigma}^\dagger c_{j\sigma} - it' \sum_{\langle\langle ij \rangle\rangle \sigma} \nu_{ij} c_{i\sigma}^\dagger c_{j\sigma} - \mu \sum_{i\sigma} c_{i\sigma}^\dagger c_{i\sigma} \tag{1}$$

and H_U is the Hubbard interaction,

$$H_U = U \sum_i n_{i\uparrow} n_{i\downarrow} \tag{2}$$

Here, $\langle ij \rangle$ and $\langle\langle ij \rangle\rangle$ denote the nearest-neighbor and the NNN bonds, respectively. $\nu_{ij} = +1(-1)$ if the electron makes a left (right) turn to get to the NNN site. μ is the chemical potential and is set to be $U/2$ due to the particle hole symmetry of the system. Others are in standard notation. Throughout this work, we use t as the energy unit. Due
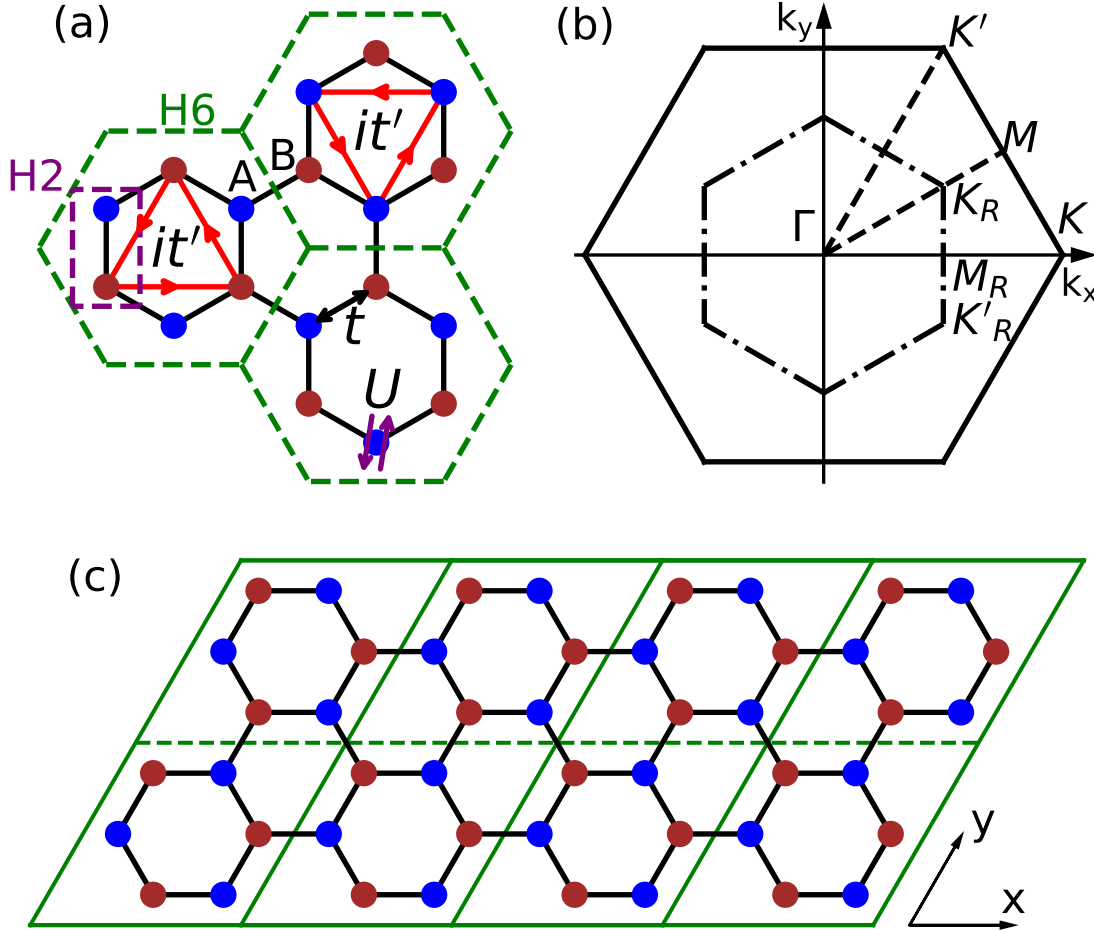
Figure 1. (color online). (a) Six-site cluster tiling as enclosed by the green dashed lines on the honeycomb lattice. The original unitcell enclosed by the purple dashed lines contains two nonequivalent sites. The hopping amplitudes t, it' and the Hubbard interaction U of the Haldane Hubbard model are also shown. (b) First Brillouin zone (FBZ) of the original lattice (black solid hexagon) and of the superlattice of the six-site cluster (black dashed hexagon). (c) An illustration of tiling the armchair ribbon used for the calculations of edge states. The superclusters (parallelogram with green solid lines) are arranged periodically along the x direction. For illustration, we only plot two clusters (separated by the green dashed line) in each supercluster, while in the calculations fifteen clusters are included along the y direction.

to the pure imaginary NNN hopping it', this model breaks the time reversal symmetry locally and there exits nonhomogeneous flux in the honeycomb lattice but the total flux through every single hexagon is zero. As a consequence, in the non-interacting limit, the ground state of the system has a nonzero Chern number and is a Chern insulator.

CPT [22] is a quantum cluster approach accessing to the single particle Green's functions of systems with only onsite interactions. In CPT, the lattice is tiled into superlattice of clusters. Each cluster is solved exactly and the inter-cluster single particle

terms are treated as perturbations. Then the single particle Green's function $G(\tilde{\mathbf{k}}, \omega)$ of the system is obtained through an RPA-like approximation:

$$G^{-1}(\tilde{\mathbf{k}}, \omega) = G_0^{-1}(\omega) - V(\tilde{\mathbf{k}}) \tag{3}$$

where $G_0(\omega)$ is the exact cluster single particle Green's function, $V(\tilde{\mathbf{k}})$ is the inter-cluster quadratic terms, and $\tilde{\mathbf{k}}$ belongs to the reduced first Brillouin zone (FBZ) of the superlattice. As is common in most quantum cluster approaches (except DCA), this tiling of superlattice usually breaks the translation symmetry, and the single particle Green's function $G_{per}(\mathbf{k}, \omega)$ in the original FBZ can be approximated by the so-called periodization procedure:

$$[G_{per}]_{\alpha\beta}(\mathbf{k}, \omega) = \frac{1}{L} \sum_{a \in \{\alpha\}, b \in \{\beta\}} G_{ab}(\mathbf{k}, \omega) \exp\left[-i\mathbf{k} \cdot (\mathbf{r}_a - \mathbf{r}_b)\right] \tag{4}$$

where L is the number of unit cells in the cluster, α (β) is a composite index of site and spin in a unit cell, and $\{\alpha\}$ ($\{\beta\}$) is the set of all equivalent indices of α (β) in the cluster with respect to the translation symmetry of the original lattice.

CPT is exact in the non-interacting limit but does not allow for spontaneous symmetry breaking phases. To find such phases, one would resort to VCA [25], which can be viewed as a variational version of CPT according to the self energy functional theory [34]. Here, the decoupled clusters with additional Weiss terms is employed as the reference system and its self-energy takes on an approximation of the original's. Then the grand potential functional can be expressed as

$$\Omega(h') = \Omega'(h') - \text{Tr} \ln \left\{ 1 - \left[g_0'^{-1}(h') - g_0^{-1} \right] G_0'(h') \right\} \tag{5}$$

where Ω (Ω') and g_0 (g_0') are the grand potential and the free propagator of the original (reference) system, respectively. G_0' is the exact cluster single particle Green's function of the reference system and h' denotes the introduced Weiss field. A symmetry-breaking phase is obtained if the grand potential $\Omega(h')$ takes a minimum at a finite value of the Weiss field.

In interacting many-body systems, the single particle Green's function is a useful tool to investigate the topological properties [11, 48, 13]. Actually, the topological Hamiltonian [14], which is defined as the minus inverse of the zero-frequency single particle Green's function, i.e.

$$H_{topo}(\mathbf{k}) = -G_{per}^{-1}(\mathbf{k}, \omega)\big|_{\omega=0} \tag{6}$$

is sufficient to encode all the topological information if the system has no nontrivial ground state degeneracies [13]. For example, the interacting Chern number can be constructed via the Kubo formula [12]

$$C = i \sum_{E_m < \mu < E_n} \int \frac{d^2\mathbf{k}}{(2\pi)^2} \frac{\langle m|v_x|n\rangle\langle n|v_y|m\rangle - \langle m|v_y|n\rangle\langle n|v_x|m\rangle}{(E_m - E_n)^2} \tag{7}$$

in terms of the topological Hamiltonian's eigenvalues E_i and eigenvectors $|i\rangle$ ($i = m, n$). Here $v_\alpha = \frac{\partial H_{topo}}{\partial k_\alpha}$ ($\alpha = x, y$) is the velocity operator.
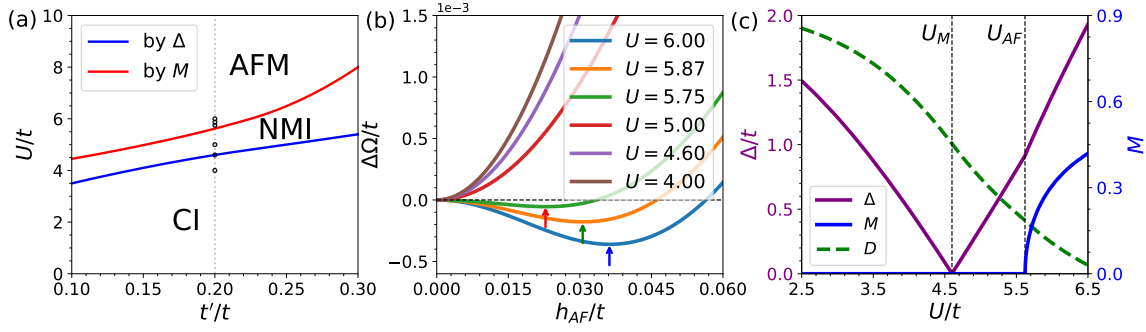
Figure 2. (color online). (a) Groundstate phase diagram of the Haldane Hubbard model. CI, NMI, and AFM denote Chern insulator, nonmagnetic Mott insulator and antiferromagnetic Mott insulator, respectively. The dotted line at $t' = 0.2$ marks the parameters used in Fig. 2(c), Fig. 3(b) and Fig. 6(b). The circles mark the parameters used in Fig. 2(b), Fig. 4, Fig. 5, and Fig. 7. (b) $\Delta\Omega$ as a function of h_{AF} for $t' = 0.2$. Arrows indicate the positions of the minima, where magnetic solutions are allowed. (c) The single particle gap Δ (purple solid line), the antiferromagnetic moment M (blue solid line) and the double occupancy D (green dashed line) as a function of U for $t' = 0.2$. $U_M = 4.60$ and $U_{AF} = 5.62$ represent the Mott transition point and the paramagnetic-antiferromagnetic transition point, respectively. We note that the double occupancy is rescaled linearly in order to plot it in the same figure.

3. Results

Our results are obtained by use of CPT/VCA on the 6-site-cluster-tiled superlattice (the superlattice is composed of 100×100 clusters) as illustrated in Fig. 1(a). This cluster not only preserves the point-group symmetry of the Hamiltonian but also has zero net flux through it, which is essential for the Haldane Hubbard model. So, it is the best choice considering the available computation capacity.

3.1. Phase diagram

Before the discussion of the interacting Chern number C, we first present the phase diagram determined by the single particle gap Δ, the antiferromagnetic (AF) moment $M = \frac{1}{N}\sum_i (-1)^{\eta_i} \langle c_{i\alpha}^\dagger \sigma_{\alpha\beta}^z c_{i\beta}\rangle$ and the double occupancy of electrons $D = \frac{1}{N}\sum_i \langle n_{i\uparrow} n_{i\downarrow}\rangle$, as shown in Fig. 2(a). Here $\eta_i = 0$ or 1 when $i \in A$ or B and N is the number of lattice sites. There are three distinct phases separated by two phase boundaries. The single particle gap keeps nonzero except on the transition line from CI to NMI while the AF moment is nonzero only for AFM.

Take $t' = 0.2$ as an example, let's have a close look at these quantities. Δ, M and D are computed at the minimum points of the grand potential Ω with respect to the Weiss field corresponding to M: $H_{AF} = h_{AF}\sum_i (-1)^{\eta_i} c_{i\alpha}^\dagger \sigma_{\alpha\beta}^z c_{i\beta}$. In Fig. 2(b), $\Delta\Omega = \Omega(h_{AF}) - \Omega(h_{AF} = 0)$ at the parameters indicated by the circles in Fig. 2(a) are shown. It is clear that for small Hubbard U, $\Delta\Omega$ takes its minimum when $h_{AF} = 0$, indicating that the system is exempt from magnetic order, while for large U, $\Delta\Omega$ reaches its minimum when h_{AF} is nonzero, meaning that the AF moment has already formed. In
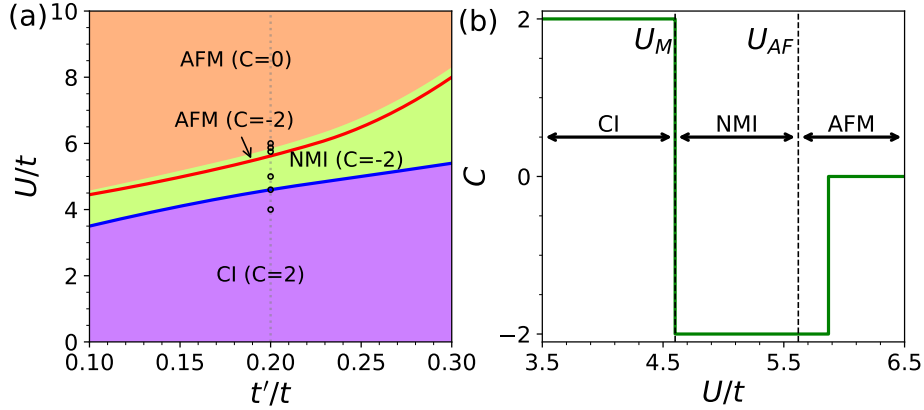
Figure 3. (color online). Generalized Chern number C with H2 being the unitcell (a) in the U-t' plane (2 for magenta, -2 for green and 0 for orange), and (b) as a function of U with $t' = 0.2$. The AFM phase contains a narrow region with a nonzero Chern number near the AFM-NMI phase boundary. The dotted line and the circles are the same to those in Fig. 2(a).

Fig. 2(c), Δ, M and D are plotted for a range of Us. With increasing U, Δ decreases at first, gets to zero at U_M, and then increases linearly, but encounters a change of the slope at U_{AF}. A rapid decrease of D occurs around U_M, specifically the inflection point of D coincides with U_M. Combining this with the linear dependency of the reopened gap with U, the transition at U_M is identified as the Mott transition. M develops continuously at U_{AF}. Therefore, the transition here is the paramagnetic-antiferromagnetic transition.

3.2. Paradox between the bulk Chern number and the edge states/zeros

Now let's turn to the interacting Chern number C of the model, which is computed in terms of Eqs. (6-7), and shown in Fig. 3(a). It is observed that the Chern number is 2 for CI and -2 for NMI, while for the AFM phase, it is -2 near the NMI-AFM phase boundary and 0 deep in the AFM phase. To see this more clearly, in Fig. 3(b), we plot C as a function of U with $t' = 0.2$. Apparently, the Chern number changes its sign across $U = U_M$ and survives a noticeable range of U after the AF order appears, and eventually alters its value from -2 to 0 at a point of $U > U_{AF}$. Therefore, it seems that there exists two successive topological phase transitions.

It is established that in the non-interacting limit, topological phase transitions cannot occur without closing the single particle gap. This also accounts for what happens at the first transition ($U = U_M$) when the interaction is not strong enough to induce an AF order in the model we study here. In the interacting regime, there are two more scenarios of topological transitions. One is the first-order transition across which the local order parameters change discontinuously [50, 40, 51], the other is the zeros-driven transition where the change of the topological invariants are due to the emergence of zero-energy zeros of the single-particle Green's functions [48, 52, 19]. Both scenarios can avoid the closing of the single particle gap. From Fig. 2(c), we can see
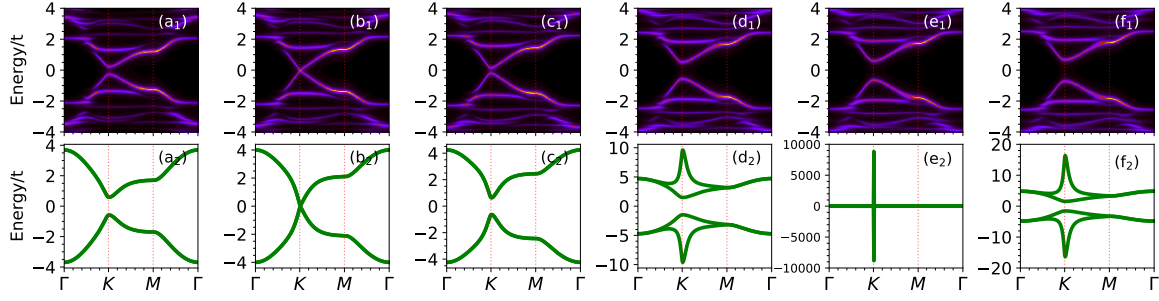
Figure 4. (color online). Intensity plot of the single particle spectra (top) and topological Hamiltonian's spectra (bottom) along the high symmetry path in the FBZ calculated with (a) $U = 4.00$, $h_{AF} = 0$, (b) $U = 4.60$, $h_{AF} = 0$, (c) $U = 5.00$, $h_{AF} = 0$, (d) $U = 5.75$, $h_{AF} = 0.0228$, (e) $U = 5.87$, $h_{AF} = 0.0306$, and (f) $U = 6.00$, $h_{AF} = 0.0362$. The values of h_{AF} are determined by the locations of $\Delta\Omega$s' minima in Fig. 2(b). The NNN hopping is fixed at $t' = 0.2$. (b) corresponds to the first change of the Chern number C in Fig. 3(b) and (e) to the second.
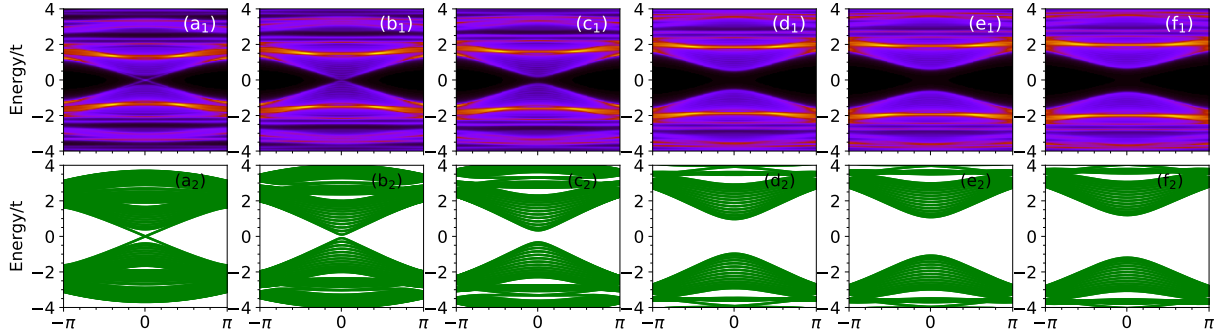

Figure 5. (color online). Intensity plot of the single particle spectra (top) and topological Hamiltonian's spectra (bottom) on the armchair ribbon illustrated in Fig. 1(c) calculated with the same parameters in Fig. 4.

that at the "second topological transition" ($U > U_{AF}$), the single particle gap Δ do not close and the AF moment M is continuous with U. Thus this transition does not belong to the first two scenarios. Then does it belong to the last scenario? To see this, in Fig. 4, we plot the single particle spectral function $A(\mathbf{k}, \omega) = -2\,ImG(\mathbf{k}, \omega + i0^+)/\pi$ and the topological Hamiltonian's spectra along a high symmetry path in the FBZ at the circled points indicated in Fig. 3(a). With increasing U, the single particle spectra and the topological Hamiltonian's spectra show a quite similar evolution before the AF moment forms [see Figs. 4(a)-(c)], namely their gaps both close at K/K' at the first transition ($U = U_M$). However, their behaviors deviate from each other essentially after the formation of the AF moment [see Figs. 4(d)-(f)]. Now, the single particle spectra exhibit few changes except that the gap increases linearly. While, the topological Hamiltonian's spectra quickly develop a divergence at K/K' when one approaches the "second topological transition" ($U > U_{AF}$).

A divergence of the spectra of the topological Hamiltonian corresponds to the emergence of a zero-energy zero of the single particle Green's functions. Now every
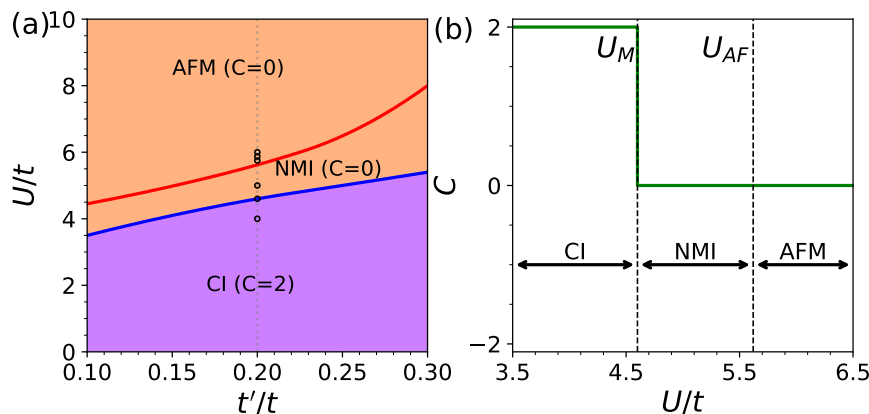
Figure 6. (color online). Generalized Chern number C with H6 being the unitcell (a) in the U-t' plane (2 for magenta, and 0 for orange), and (b) as a function of U with $t' = 0.2$. Both the NMI phase and the AFM phase acquire zero Chern number. The dotted line and the circles are the same to those in Fig. 2(a).

evidence seems to lead us to a conclusion that the "second topological transition" at $U > U_{AF}$ is a concrete realization in a microscopic model of the last scenario, as was similarly claimed in Ref. [35]. But wait. According to the generalized bulk-edge correspondence [48, 49], a topological phase with a nonzero interacting bulk Chern number must assume gapless single particle states or zero-energy zeros of the single particle Green's function on open boundaries. To check this, in Fig. 5, we plot the single particle spectral and the topological Hamiltonian's spectra with the same parameters as those in Fig. 4 on an armchair ribbon as illustrated in Fig. 1(c). In order to completely tile the stripe, a 6-site cluster is used. In our calculations, fifteen clusters are included in the y direction to form a supercluster and the superclusters are arranged periodically in the x direction. For illustration, we only show schematically two clusters in the y direction in Fig. 1(c). It is clear that before the first transition at $U = U_M$, for both the single particle spectra and the topological Hamiltonian's spectra, there always exist gapless edge modes [see Fig. 5(a)]. However, after this transition, we cannot observe any gapless edge state or any zero-energy zero of the single particle Green's function [see Figs. 5(c)-(f)], even for those with a nonzero bulk Chern number [see Figs. 5(c)-(d)]. So what's going wrong?

3.3. Falsity of the bulk Chern number

To resolve this paradox, let's enumerate the approximations we make in our quantum cluster calculations. First, the self-energy of the real system is replaced by that of a reference system, and second, the single particle Green's functions in the original Brillouin zone are approximated by a periodization procedure. For the model we study here subject to both periodic and open boundary conditions, their reference systems are the same, but the the periodization procedure is needed for the periodic boundary condition while it is not for the open boundary condition. This procedure aims to restore
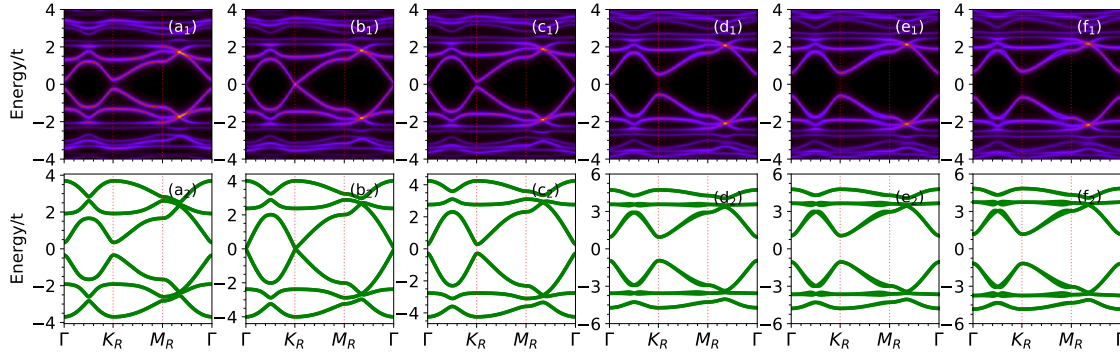
Figure 7. (color online). Intensity plot of the single particle spectra (top) and topological Hamiltonian's spectra (bottom) along the high symmetry path in the reduced FBZ calculated with the same parameters in Figs. 4-5.

the explicitly broken translation symmetry of the original lattice but now is suspectable to be responsible for this paradox.

The above conjecture is supported by the following argument. Assume the original system is disturbed by a small local perturbation ΔH such that the translation symmetry is broken and the new unit cell is exactly the six-site cluster as shown in Fig. 1(a). A real topological phase with a nonzero Chern number should be stable against such small perturbations, which means the new Chern number of the disturbed phase should remain unchanged. Note that the computation process for this new Chern number by our quantum cluster approaches is exactly the same with that in Sec. 3.2, except that the periodization procedure is not needed any more. Now let ΔH approach 0. The $\Delta H = 0+$ limiting case can be viewed as the same with the original system, but with a larger six-site unit cell. However, as shown in Fig. 6(a), the Chern number in the moderate interacting regime for this limiting system exhibits quite different behaviors compared to those shown in Sec. 3.2. Specifically, there exist only one change of C that occurs at the Mott transition point U_M, and after this transition, C always remains 0, which can be seen more clearly in Fig. 6(b). The "second topological transition" simply disappears. In Fig. 7, we also plot the single particle spectra and the topological Hamiltonian's spectra of this limiting case with the same parameters as those in Fig. 4. It can be seen that although both spectra still close their gaps at U_M [see Fig. 4(b) and Fig. 7(b)], the divergence of the topological Hamiltonian's spectra does not emerge after the AF moment develops [see Fig. 4(e) and Fig. 7(e)]. The only difference between the original system and the limiting system is that the latter avoids the approximation of the periodization procedure. Moreover, the latter result is consistent with those with open boundaries shown in Fig. 5 while the former is not. Therefore, we conclude that the nontriviality of the Chern number of the intermediate phases shown in Sec. 3.2 and Ref. [35] is just an artifact of the breaking of the translation symmetry which is hard coded in the periodization procedure of quantum cluster approaches.

Finally, we note that the Chern number of the CI phase with weak interactions is stable against the approximation of the periodization procedure. However, no a priori

judgement can be made on whether the calculated Chern number is reliable if we do not resort to the single particle spectra and the topological Hamiltonian's spectra on open boundaries. We thus assert that a faithful verification of a nontrivial topological phase in correlated Chern insulators by quantum cluster approaches must combine both, i.e. a nonzero interacting bulk topological invariant and the existence of gapless edge states or zero-energy edge zeros of the single particle Green's functions.

4. Summary and discussion

In summary, with investigations on the Haldane Hubbard model as the prototype, we have uncovered the unexpected possible falsity of the interacting topological invariants computed by quantum cluster approaches in correlated Chern insulators. This falsity is deeply related to the explicit breaking of the translation symmetry which is universal for most quantum cluster approaches. We assert that a faithful verification of a nontrivial topological phase in correlated Chern insulators by quantum cluster approaches must combine a nonzero interacting bulk topological invariant and the existence of gapless edge states or zero-energy edge zeros of the single particle Green's functions.

We want to remark that the actual phase diagram of the Haldane Hubbard model in the moderate interacting regime has been highly debated over the past several years, but different methods predicted quite different results [36, 37, 38, 39, 40, 41, 42, 43, 44, 45, 46, 47]. In particular, even whether the intermediate phases exist has not come to an agreement, let alone their physical properties. Due to the limited power of quantum cluster approaches, we aim no settlement of this difficult problem in this paper. However, it is safe to claim that in the framework of CPT/VCA, the intermediate phase (NMI) exists and it is not topological in the sense that it has no nonzero interacting bulk Chern number nor gapless states or zero-energy zeros of the single particle Green's function on edges. Besides, the spinless free Haldane model has been realized in recent cold atom experiments using the shaking lattice technique [53]. We hope our claim can be tested in future experiments.

Acknowledgement

References

[1] M. Z. Hasan and C. L. Kane. Colloquium: Topological insulators. *Rev. Mod. Phys.*, 82(4):3045–3067, nov 2010.
[2] Xiao-Liang Qi and Shou-Cheng Zhang. Topological insulators and superconductors. *Rev. Mod. Phys.*, 83:1057–1110, Oct 2011.

[3] F. D. M. Haldane. Model for a quantum hall effect without landau levels: Condensed-matter realization of the "parity anomaly". *Phys. Rev. Lett.*, 61:2015–2018, Oct 1988.

[4] A Yu Kitaev. Unpaired majorana fermions in quantum wires. *Phys. Usp.*, 44(10S):131–136, oct 2001.

[5] C. L. Kane and E. J. Mele. Quantum spin hall effect in graphene. *Phys. Rev. Lett.*, 95(22):226801, nov 2005.

[6] B. A. Bernevig, T. L. Hughes, and S.-C. Zhang. Quantum spin hall effect and topological phase transition in HgTe quantum wells. *Science*, 314(5806):1757–1761, dec 2006.

[7] Kai Li, Shun-Li Yu, Zhao-Long Gu, and Jian-Xin Li. Phase diagram and topological phases in the triangular lattice kitaev-hubbard model. *Phys. Rev. B*, 94(12):125120, sep 2016.

[8] Jin-Guo Liu, Zhao-Long Gu, Jian-Xin Li, and Qiang-Hua Wang. Local indistinguishability and edge modes revealed by the sub-system fidelity. *New J. Phys.*, 19(9):093017, sep 2017.

[9] Xiao-Liang Qi, Yong-Shi Wu, and Shou-Cheng Zhang. General theorem relating the bulk topological number to edge states in two-dimensional insulators. *Phys. Rev. B*, 74(4):045125, jul 2006.

[10] Andreas P. Schnyder, Shinsei Ryu, Akira Furusaki, and Andreas W. W. Ludwig. Classification of topological insulators and superconductors in three spatial dimensions. *Phys. Rev. B*, 78(19):195125, nov 2008.

[11] G. E. Volovik. The universe in a helium droplet., 2003.

[12] D. J. Thouless, M. Kohmoto, M. P. Nightingale, and M. den Nijs. Quantized hall conductance in a two-dimensional periodic potential. *Phys. Rev. Lett.*, 49:405–408, Aug 1982.

[13] Zhong Wang and Shou-Cheng Zhang. Simplified topological invariants for interacting insulators. *Phys. Rev. X*, 2(3):031008, Aug 2012.

[14] Zhong Wang and Binghai Yan. Topological hamiltonian as an exact tool for topological invariants. *J. Phys. Condens. Matter*, 25(15):155601, 2013.

[15] Jan Werner and Fakher F. Assaad. Interaction-driven transition between topological states in a kondo insulator. *Phys. Rev. B*, 88(3):035113, jul 2013.

[16] Thomas C. Lang, Andrew M. Essin, Victor Gurarie, and Stefan Wessel. Z2 topological invariants in two dimensions from quantum monte carlo. *Phys. Rev. B*, 87(20):205101, may 2013.

[17] F Grandi, F Manghi, O Corradini, C M Bertoni, and A Bonini. Topological invariants in interacting quantum spin hall: a cluster perturbation theory approach. *New J. Phys.*, 17(2):023004, 2015.

[18] Xiancong Lu and D. Sénéchal. Parity-mixing superconducting phase in the rashba-hubbard model and its topological properties from dynamical mean-field theory. *Phys. Rev. B*, 98(24):245118, dec 2018.

[19] Bjrn Sbierski and Christoph Karrasch. Topological invariants for the haldane phase of interacting su-schrieffer-heeger chains: Functional renormalization-group approach. *Phys. Rev. B*, 98(16):165101, oct 2018.

[20] Thomas Maier, Mark Jarrell, Thomas Pruschke, and Matthias H. Hettler. Quantum cluster theories. *Rev. Mod. Phys.*, 77(3):1027–1080, oct 2005.

[21] David Sénéchal. An introduction to quantum cluster methods. *arXiv:0806.2690*, 2008.

[22] D. Sénéchal, D. Perez, and M. Pioro-Ladrière. Spectral weight of the hubbard model through cluster perturbation theory. *Phys. Rev. Lett.*, 84:522–525, Jan 2000.

[23] M. H. Hettler, M. Mukherjee, M. Jarrell, and H. R. Krishnamurthy. Dynamical cluster approximation: Nonlocal dynamics of correlated electron systems. *Phys. Rev. B*, 61(19):12739–12756, may 2000.

[24] Gabriel Kotliar, Sergej Y. Savrasov, Gunnar Pálsson, and Giulio Biroli. Cellular dynamical mean field approach to strongly correlated systems. *Phys. Rev. Lett.*, 87(18):186401, oct 2001.

[25] M. Potthoff, M. Aichhorn, and C. Dahnken. Variational cluster approach to correlated electron systems in low dimensions. *Phys. Rev. Lett.*, 91(20):206402, Nov 2003.

[26] M. Balzer, B. Kyung, D. Sénéchal, A.-M. S. Tremblay, and M. Potthoff. First-order mott

transition at zero temperature in two dimensions: Variational plaquette study. *Europhys. Lett.*, 85(1):17002, jan 2009.

[27] Jing Kang, Shun-Li Yu, Tao Xiang, and Jian-Xin Li. Pseudogap and fermi arc in κ-type organic superconductors. *Phys. Rev. B*, 84(6):064520, Aug 2011.

[28] Shun-Li Yu, X. C. Xie, and Jian-Xin Li. Mott physics and topological phase transition in correlated dirac fermions. *Phys. Rev. Lett.*, 107(1):010401, Jun 2011.

[29] Shun-Li Yu and Jian-Xin Li. Chiral superconducting phase and chiral spin-density-wave phase in a hubbard model on the kagome lattice. *Phys. Rev. B*, 85(14):144402, Apr 2012.

[30] Weng-Hang Leong, Shun-Li Yu, T. Xiang, and Jian-Xin Li. Localized in-gap state in a single-electron doped mott insulator. *Phys. Rev. B*, 90(24):245102, Dec 2014.

[31] W Koller and N Dupuis. Variational cluster perturbation theory for bose–hubbard models. *J. Phys. Condens. Matter*, 18(41):9525–9540, sep 2006.

[32] Michael Knap, Enrico Arrigoni, and Wolfgang von der Linden. Variational cluster approach for strongly correlated lattice bosons in the superfluid phase. *Phys. Rev. B*, 83(13):134507, apr 2011.

[33] Shun-Li Yu, Wei Wang, Zhao-Yang Dong, Zi-Jian Yao, and Jian-Xin Li. Deconfinement of spinons in frustrated spin systems: Spectral perspective. *Phys. Rev. B*, 98(13):134410, oct 2018.

[34] Michael Potthoff. Self-energy-functional approach to systems of correlated electrons. *Eur. Phys. J. B*, 32(4):429–436, 2003.

[35] Jingxiang Wu, Jean Paul Latyr Faye, David Sénéchal, and Joseph Maciejko. Quantum cluster approach to the spinful haldane-hubbard model. *Phys. Rev. B*, 93(7):075131, feb 2016.

[36] Jing He, Yan-Hua Zong, Su-Peng Kou, Ying Liang, and Shiping Feng. Topological spin density waves in the hubbard model on a honeycomb lattice. *Phys. Rev. B*, 84(3):035127, Jul 2011.

[37] Jing He, Su-Peng Kou, Ying Liang, and Shiping Feng. Chiral spin liquid in a correlated topological insulator. *Phys. Rev. B*, 83(20):205116, May 2011.

[38] Joseph Maciejko and Andreas Rüegg. Topological order in a correlated chern insulator. *Phys. Rev. B*, 88(24):241101, Dec 2013.

[39] C. Hickey, P. Rath, and A. Paramekanti. Competing chiral orders in the topological haldane-hubbard model of spin-$\frac{1}{2}$ fermions and bosons. *Phys. Rev. B*, 91(13):134414, Apr 2015.

[40] Wei Zheng, Huitao Shen, Zhong Wang, and Hui Zhai. Magnetic-order-driven topological transition in the haldane-hubbard model. *Phys. Rev. B*, 91(16):161107, Apr 2015.

[41] Ciarán Hickey, Lukasz Cincio, Zlatko Papić, and Arun Paramekanti. Haldane-hubbard mott insulator: From tetrahedral spin crystal to chiral spin liquid. *Phys. Rev. Lett.*, 116(13):137202, apr 2016.

[42] Tuomas I. Vanhala, Topi Siro, Long Liang, Matthias Troyer, Ari Harju, and Pivi Trm. Topological phase transitions in the repulsively interacting haldane-hubbard model. *Phys. Rev. Lett.*, 116(22):225305, jun 2016.

[43] Jakub Imriška, Lei Wang, and Matthias Troyer. First-order topological phase transition of the haldane-hubbard model. *Phys. Rev. B*, 94(3):035109, jul 2016.

[44] V. S. Arun, R. Sohal, C. Hickey, and A. Paramekanti. Mean field study of the topological haldane-hubbard model of spin-12fermions. *Phys. Rev. B*, 93(11):115110, mar 2016.

[45] Alessandro Giuliani, Ian Jauslin, Vieri Mastropietro, and Marcello Porta. Topological phase transitions and universality in the haldane-hubbard model. *Phys. Rev.B*, 94(20):205139, nov 2016.

[46] A Rubio-García and J J García-Ripoll. Topological phases in the haldane model with spin–spin on-site interactions. *New J. Phys.*, 20(4):043033, apr 2018.

[47] Duc-Anh Le, Minh-Tien Tran, Thi-Thanh-Mai Tran, Thi-Thao Nguyen, Thi-Huong Nguyen, and Anh-Tuan Hoang. Phase transitions in the haldane-hubbard model within coherent potential approximation. *Phys. B Condens. Matter*, 532:139–143, mar 2018.

[48] V. Gurarie. Single-particle green's functions and interacting topological insulators. *Phys. Rev. B*, 83(8):085426, Feb 2011.

[49] Andrew M. Essin and Victor Gurarie. Bulk-boundary correspondence of topological insulators from their respective green's functions. *Phys. Rev. B*, 84(12):125132, sep 2011.

[50] Jan Carl Budich, Bjrn Trauzettel, and Giorgio Sangiovanni. Fluctuation-driven topological hund insulators. *Phys. Rev. B*, 87(23):235104, jun 2013.

[51] A. Amaricci, J.C. Budich, M. Capone, B. Trauzettel, and G. Sangiovanni. First-order character and observable signatures of topological quantum phase transitions. *Phys. Rev. Lett.*, 114(18):185701, may 2015.

[52] Jan Carl Budich, Ronny Thomale, Gang Li, Manuel Laubach, and Shou-Cheng Zhang. Fluctuation-induced topological quantum phase transitions in quantum spin-hall and anomalous-hall insulators. *Phys. Rev. B*, 86(20):201407, nov 2012.

[53] Gregor Jotzu, Michael Messer, Rémi Desbuquois, Martin Lebrat, Thomas Uehlinger, Daniel Greif, and Tilman Esslinger. Experimental realization of the topological haldane model with ultracold fermions. *Nature*, 515(7526):237–240, 2014.